Flow Measurement and Instrumentation 100 (2024) 102718

Contents lists available at ScienceDirect

Flow Measurement and Instrumentation

journal homepage: www.elsevier.com/locate/flowmeasinst

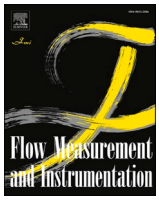

Hydraulic valve design methodology for hydro turbine control system

Mateusz Kosek [a,*], Dariusz Downar [a,1], Pawel Sliwinski [b,1]

[a] Instytut Energetyki – Państwowy Instytut Badawczy, 01-330, Warszawa, Mory 8, Oddzial Gdansk, Poland
[b] Division of Hydraulics and Pneumatics, Faculty of Mechanical Engineering and Ship Technology, Gdansk University of Technology, ul. Gabriela Narutowicza 11/12, 80-233, Gdansk, Poland

ARTICLE INFO

Keywords:
Hydraulic valve
Proportional flow control valve
CFD
Validation of numerical calculations
Hydropower

ABSTRACT

The control of the turbine and its equipment in a hydroelectric power plant requires the HPU (hydraulic power unit) to deliver large volumes of working fluid in a short time at specific optimum control parameters. The use of typical proportional flow control valves created by manufacturers of hydraulic components in low-pressure control systems is disadvantageous due to high pressure losses in the control chambers. This paper presents the methodology and test results while designing a hydraulic proportional valve for low pressure and high flow rate operation. CFD (computational fluid dynamics) theory was analyzed and characteristic values were determined. The validation of CFD tests through those on the test bench was carried out, correction factor was determined. A new proprietary solution was developed and a series of simulation studies were carried out to determine the flow characteristics depending on the degree of the opening of the proportional flow control valve.

1. Introduction

Mechanical control systems based on power hydraulics are used to control the operation of hydro turbine [1,2] by the actuators. General diagram of HPU of hydro turbine (Kaplan type [3,4]) is shown in Fig. 1. HPU systems are used due to their ability to generate enormous forces while ensuring compact system development, reliable operation and virtually no compressibility of the working medium. The elements that control the direct position of the actuators of hydro-units, i.e. the wicket gate and rotor blades are hydraulic actuators - usually double-acting. This means that the direction of movement of the actuators is changed by changing the connection of the actuator ports - one of them must be supplied with the pressurized working medium, while the other one must be deprived of it. Proportional flow control valves are usually used to control the direction of the movement of the hydraulic receivers. Hydro turbine (Kaplan type) have a special correlation between the given opening of the wicket gate and the rotor blades - called cam curves characteristics. Turbine control requires reliable and precise operation of the hydraulic power unit in various operating modes. Each of these operating modes takes place at a different point in the cam curves characteristics of the turbine set, i.e. at different openings of the wicket gate and the rotor blades. This is usually the consequence of different values of hydraulic forces acting on the wicket gate blades and the rotor blades due to the flowing water (or only on wicket gate blades in the case of Francis hydro turbine). As mentioned earlier, it is required to maintain a constant rotational speed (except start-up and shutdown operation mode). The current position of the wicket gate actuators and the rotor blades is usually measured with the use of magneto strictive linear position transducers. In order to achieve the appropriate set value for opening the actuators of the turbine set in a short time, proportional flow control valves are used in the hydraulic units controlling the wicket gate and rotor blades actuators (elements of the HPU system). These are proportional flow control valves equipped with a control coil, where thanks to the built-in valve electronics and the measurement of the spool position, it is possible to control the opening value of this valve within a specific range, using a specific control signal. The use of the proportional technique assumes that the flow rate at a given pressure drop is proportional to the control signal. In high flow rate hydraulic systems are usually used to control two stage proportional flow control valves. This kind of valve unit consists of two valves.

- the bigger one which controls the flow rate to the receiver;
- the smaller one for control the opening of the bigger valve spool.

This type of construction allows the use of hydraulic amplification and the use of a much smaller control coil. This improves the dynamics

* Corresponding author.
E-mail address: m.kosek@ien.gda.pl (M. Kosek).
[1] These authors contributed equally to this work. These authors jointly supervised this work.

https://doi.org/10.1016/j.flowmeasinst.2024.102718
Received 27 June 2024; Received in revised form 25 September 2024; Accepted 14 October 2024
Available online 16 October 2024

of the hydraulic valve and is much less energy-consuming.

The main goal of the work is to create a hydraulic proportional flow control valve assembly that controls the position of the steering actuators of the wicket gate and the blade runner of the hydro unit. The work has been divided into two stages. The first one describes the process of designing the low-pressure high flow rate main proportional flow control valve, which is described in this publication. The second stage involves the development of a high-pressure element (pilot valve) controlling the main control valve.

1.1. Characteristics of the commercial elements

Many manufacturers of hydraulic components such as Bosch-Rexroth [5], Hydac, Eaton, Yukon, Ponar Wadowice produce directional control valves in proportional technology. Typically, most manufacturers produce components in the mechanical size 4–25. Few manufacturers produce components for sizes 27–35. Virtually all series of the produced components are suitable for the use in high-pressure hydraulic systems, where system operating pressures typically exceed $100{\cdot}10^5$ Pa. When using commercial components in low-pressure, high-flow circuits of hydro turbine control systems, the pressure losses in the flow control components are very high. The load-dependent flow rate characteristics for different versions is shown in Fig. 2:

However, there are research papers [6,7] that show studies of the flow characteristics of commercial proportional valves, where non-linearities and incomplete proportionality of the flow rate depending on the degree of the opening are observed. Usually, the commercial proportional valves don't have a hydraulic proportionality of flow rate of spool opening function, but the proportionality of flow rate is achieved by an electronic controller. The control signal is usually in the range 4–20 mA of current and gives a linear flow characteristics, proportional to this signal.

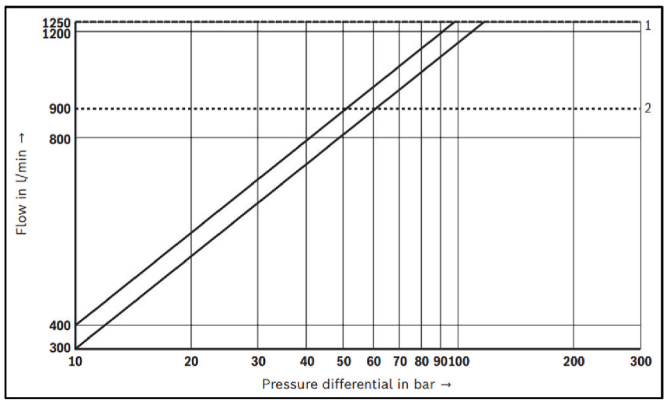

Fig. 2. Load-dependent flow rate characteristics of NG25 proportional flow control valve [5].

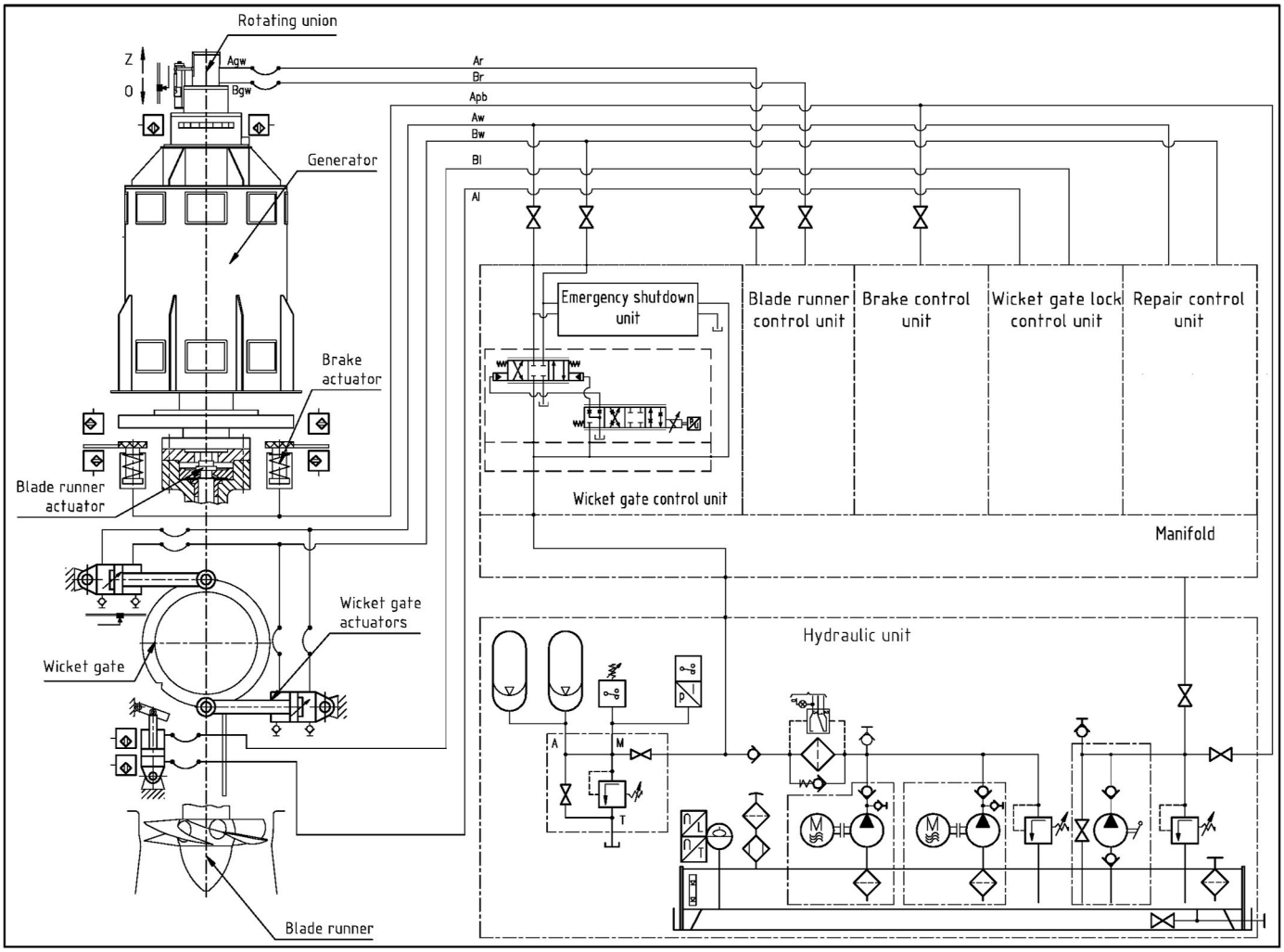

Fig. 1. General diagram of Kaplan turbine hydraulic control unit.

1.2. Proportional flow control valves currently used in the turbine HPU

There are solutions in which hydro turbine manufacturers used non-standard control elements in the HPU systems, they provided. Typically, these are elements that have been in use since the 1950s or are based on them. The proportional flow control valve spool has a very large diameter and a simple shape. There are solutions in which there are no relief grooves on the cylindrical surfaces of the spool, which leads to off-axis operation of the element in the sleeve and its faster degradation. As a consequence, this may lead to a dangerous failure of the hydro turbine control system and the inability to close the wicket gate. These valves are characterized by a very large clearance between the spool and the sleeve. As a result, there are very large internal oil leaks through the proportional flow control valve. Due to the size of the spool, there is also a very high inertia when controlling such an element. There are still many power plants of this type in operation around the world and new systems based on such solutions may be created. Typically, the failure of such an element in a single unit leads to a shutdown for several weeks and the lack of operational capabilities of the hydro unit. Hence, there was a need to design a new solution, typically for the use in low-pressure hydro-turbine HPU systems.

1.3. Menter SST k-ω turbulent model

For a better understanding of the work described in next parts of the article, issues related to CFD theory will be presented in this chapter. The model adopted to the CFD calculations was SST (shear stress transport) described below.

The results for the k-ε computational models are much less sensitive to assumed values in the free stream, but its near-wall [8] performance is unsatisfactory for near-wall layers with unfavorable pressure gradients. A hybrid model using the transformation of the k-ε model into the k-ω model in the near-wall region and a standard k-ε model in the fully turbulent far-wall region have been developed. The Reynolds stress calculation and the turbulent kinetic energy k equation are the same as in the original Wilcox k-ω model, but the rate of viscous dissipation ε equation is transformed into the turbulence frequency ω equation by the substitution [9]:

$$\varepsilon = k \bullet \omega \tag{1}$$

A comparison with the rate of turbulent kinetic energy generation shows that SST model formula has an additional source of the cross-diffusion component, which arises during the transformation of the diffusion component in the ε equation. Summarized a series of modifications aiming at the optimization of the performance of the SST k-ω model based on experiments with the model in general purpose calculations.

The main improvements are model constants and using mixing functions C. Instabilities in numerical calculations can be caused by differences in calculated vortex viscosity values with the standard k-ε model in the far field and the transformed k-ε model near the wall. Mixing functions are used to achieve a smooth transition between the two models. The mixing functions are introduced in the equation, modify the cross-diffusion term and are also used for the model constants, which take the value C1 for the original k-ω model and the value C2 in the transformed k-ε Menter model (2). Mixing function [9] $F_c = F_c\left(\frac{\iota_t}{y}, Re_y\right)$ is a function of the ratio of the turbulence ι_t (3) and the distance y to the wall and the Reynolds number Re_y (4) of the turbulence.

$$C = F_C \bullet C_1 + (1 - F_C) \bullet C_2 \tag{2}$$

$$\iota_t = \frac{\sqrt{\kappa}}{\omega} \tag{3}$$

$$Re_y = \frac{y^2 \bullet \omega}{\nu} \tag{4}$$

where: v – kinematic viscosity of the fluid.

The functional form of the Fc is adjusted in such a way that it is zero at the wall, it tends towards unity in the far field and it results in a smooth transition around half of the distance between the wall and the edge of the boundary layer. Thus, the method now combines good behavior of the k-ε model at the wall with the robustness of the k-ε model in the far field in a numerically stable way. Constraints for the SST model: vortex viscosity is limited to provide better performance in flows with unfavorable pressure gradients and wake areas, and turbulent kinetic energy generation is limited to prevent turbulence build-up in stagnant areas.

The complexity of the calculation models and their number clearly does not allow to identify a universal model or one that will present results close to the real solution in a given field. Researchers often analyse the use of multiple computational models in their publications and according to specific criteria, try to identify the most suitable one for their application. In the publication 'Analysis of Flow Characteristics and Effects of Turbulence Models for the Butterfly Valve [10]' the authors analyzed the flow characteristics and turbulence effects inside a butterfly valve using three computational models.

- k-ε,
- k-ω,
- SST.

The results of the research most converging to the exact solution (obtained experimentally) were obtained for the k-ε and SST calculation model. The highest convergence for a number of elements of about 45,000 is related to the convergence of the finite element mesh. The researchers report that the biggest kinetic turbulence energy effect was achieved by the k-ω model, followed by the SST. This is due to the fact that the biggest turbulence effect occurs in areas of high pressure drop and rapid velocity increase. This is important for the development of this project due to the fact that such phenomena occur at the control edges of the calculated valves. It is an important fact for the SST model to determine appropriate values for the first boundary layer in order to fulfill the boundary layer law.

The authors of the article [11] carried out an analysis of the three calculation models indicated earlier to determine the maximum gas flow rate through the safety valve. Due to the difference in mass flow rate results not exceeding 5 %, the authors decided to use the k-ω model, as simulation results were obtained in less than 40 % of the time (compared to the SST model). Fig. 3 also shows the results of the mesh convergence test for several variants of the number of finite elements in the model.

As the above illustration shows, the values of the quantities tested reach a practically negligible increase in value for the number of finite element exceeding 3,4 million.

The influence of the value of the height of the first wall layer and the growth factor are presented in publication [12]. The researchers analyzed the flow of the fluid through the geometry of a straight section of the pipe to determine the values of the height of the first wall layer for which the wall layer profile for turbulent flow achieves the optimum shape. The influence of the y + value on the velocity profile as a function of the height of the first boundary layer allows the indication of the erroneous turbulence profiles of the boundary layer. The results obtained indicated that the incorrect velocity profile occurs for values of y+>5 and the worst profile is obtained for a finite element mesh without an influence layer. The fact of the use of the computational model used is also important in this issue, as different computational models require different values of y + for correct near-wall turbulence profiles. Determining the correct height of the first near-wall layer is important for the proportional flow control valve issue under study. A critical element of

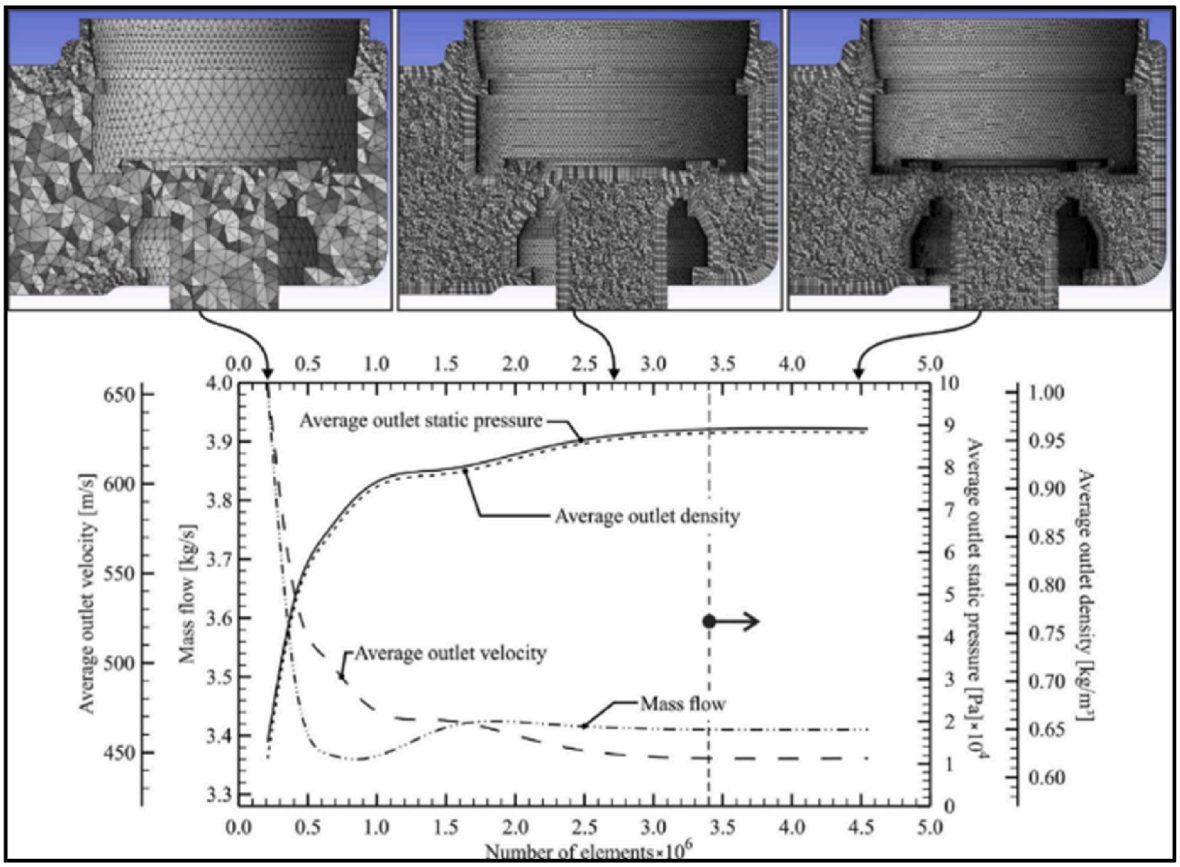

Fig. 3. Calculation results for the following boundary conditions: average outlet velocity, average outlet static pressure, mass flow and average outlet gas density [11].

the model are geometric edges of the flow window, which are formed by the positioning of the spool in the flow valve sleeve. This is the area of occurrence of the largest velocity gradients of the point under consideration, in the X,Y,Z axis direction.

The importance of the effect of determining the correct value of the height of the first wall layer on the total pressure drop of the fluid flowing through the element is described in the article [13]. The author compares the effect of the size of the first wall layer and the number of layers on the sensitivity of the finite element mesh. The output parameter is the achieved pressure drop Δp during the flow through the element, which consequently affects the mass flow achieved in the model. The results show that the calculation error was almost 17 % for the least sensitive finite element mesh - quite a difference from the reference value. This publication shows how important it is to determine the appropriate size of the first wall layer - in the case of this study, the critical area will be the control edges of the main proportional flow control valve.

It is important to determine the correct flow rate resulting from the construction of the discrete model, to ensure a favourable ratio of calculation time to the maximum flow rate achieved. Determining the correct values of the size of the first boundary layer, the number of boundary layers, the correct size of finite elements and achieving the correct parameters of the finite element mesh quality such as orthogonal quality is extremely important. Thanks to this, we can be sure of the obtained results and confirm them during laboratory tests of the prototype. The selection of the appropriate turbulence model is also important due to the fact that in a proportional flow control valve, the flow is important both in the flow channel axis and on the distributor throttle edges, where the parameters of the boundary layer have a very strong influence on the results obtained for the entire model.

2. Results of experimental tests and numerical calculations of the existing proportional flow control valve

At this section were consider methodology of building a numerical model of existing main proportional flow control valve and CFD calculation were proceed for validation of research results and uncertainty coefficient was calculated. Experiences of this research were used in calculation of newly designed proportional flow control valve. In his way, the possibilities of the available laboratory infrastructure have been checked. Performance of these tests allowed comparing the capacity of the newly developed solution with that currently used one, presented later in this manuscript.

2.1. *Tested proportional flow control valve – subject of study*

A 3D geometrical model of the investigated object was created on the basis of the documentation of an actual component stand located in the laboratory of the Institute of Power Engineering Gdansk division. Outer diameter of the spool (Fig. 4) is between 0,142-0,15 m. The difference in the diameters of the spool control surfaces results from the fact that in the event in case of loss of control pressure (usually in emergency situations of hydro-unit operation), an imbalance of forces acting on the spool occurs. The spool in the valve assumes the extreme position where the connection of the flow chambers causes the movement of the actuators for specified direction. In the emergency situations the wicket gate closes at specified speed. The geometric models were created in the CAD 3D software SolidWorks 2020 based on the old documentation. Elements and chambers of main proportional flow control valve are shown in Fig. 4. Possible connections of internal canals.

- all ports are cut-off;

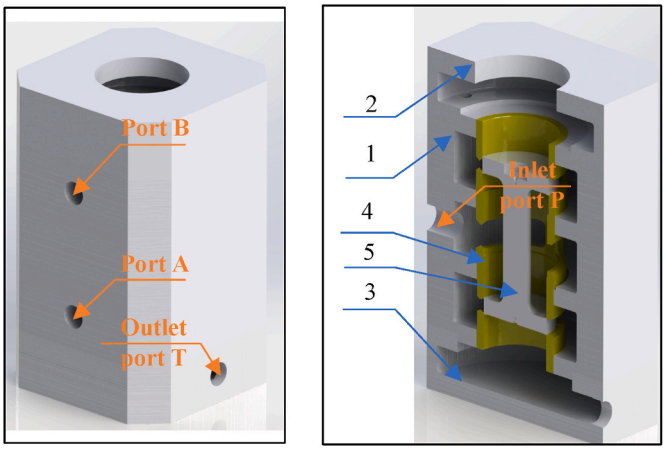

Fig. 4. Cross-section of the main proportional flow control valve. Components: 1. body, 2. top cover, 3. bottom cover, 4. sleeve, 5. spool.

- inlet port P connection to the port B, port A connection to the outflow port T;
- inlet port P connection to the port A, port B connection to the outflow port T.

2.2. Fluid geometry model

Using the intersection operation [14] for the selected geometry and the closing surfaces of the valve body, the fluid geometry containing all the flow chambers has been reconstructed (shown in Fig. 5). The resulting geometry constitutes the area to be discretized in the next step of building the computational model.

The calculations in further part of this dissertation will be carried out for the flow geometry of the connected P-B ports over the opening range of 0,001 to 0,004 m (25–100 % of the spool opening). The geometry has been parameterized to represent the change in spool position over this range. The CFD calculations were carried out in Ansys Workbench [15], the Design Modeler module was used to work with the geometry (Fig. 6), the MESH module was used for meshing, the Parameters module was used to create and use parameterizations, the CFX-PRE module was used to create boundary conditions, the calculations were carried out in CFX-Solver and the processing of the results was done in the CFD-POST module. The geometry created was exported to Ansys Workbench. Thanks to the use of the active CAD software plug-in, parameter changes made in the CAD model or in the design modeler have been updated at all locations.

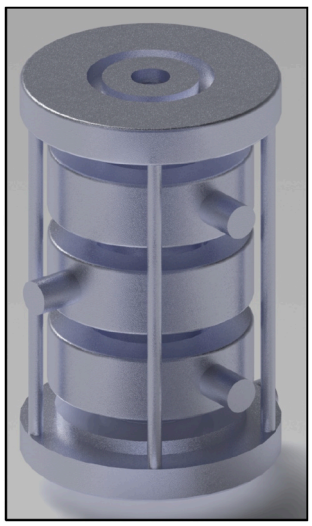

Fig. 5. Created fluid geometry.

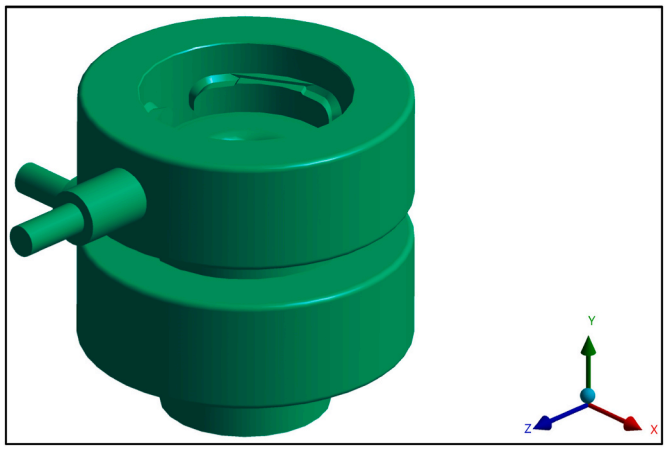

Fig. 6. Exported geometry of P-B flow ports.

2.3. Boundary conditions and parameters

While simulating an incompressible fluid for pressure inlet/pressure outlet boundary conditions, a reverse flow effect occurs. This effect is caused by uncontrolled energy inflow into the domain. Vortices are created, which cause kinetic energy instability in the computational model. A solution to this problem can be to artificially increase the size of the computational domain so that the vortices are dispersed before reaching the outflow boundary. The methodology for performing CFD calculations for pressure inlet/pressure outlet boundary conditions for an incompressible medium is described in the chapter "Proposal for a new proportional flow control valve design" and in the conclusions.

The simulation boundary conditions were determined as follows.

- the flow is isothermal, with no heat exchange;
- to slip wall;
- defined fluid model (described below);
- the calculation model used - SST (Shear Stress Transport) as described in discussion section;
- one fluid domain was defined, combining the P and B ports of the valve;
- the residual values of the calculation are RMS (Root Mean Square) $1 \bullet e^{-4}$;
- the inlet boundary is the fluid velocity, dependent from the spool opening in the range of 0,3–4,5 m/s;
- the outlet boundary is a static pressure of 0 Pa;

The physic-chemical properties of the domain were determined as for HV-32 hydraulic oil. Selected fluid parameters.

- density 840 kg/m^3,
- molar mass: 0,495 kg/mol,
- thermal capacity: 2100 J/kg•K,
- dynamic viscosity: 0,02688 Pa s,
- thermal conductivity; 0,292 W/m•K.

2.4. Mesh model and sensitivity test

Element discretization was carried out basing on patch conforming method using tetrahedral elements (tetra). The sizing of the first wall layer was done using the 'inflation' option according to the scheme in Fig. 7.

The maximum number of adjacent layers "maximum layers" was defined as 10. The growth rate of subsequent layers "Growth Rate" was

Details of "Inflation" - Inflation	
Scope	
Scoping Method	Geometry Selection
Geometry	1 Body
Definition	
Suppressed	No
Boundary Scoping Method	Geometry Selection
Boundary	1 Face
Inflation Option	First Layer Thickness
First Layer Height	5,e-002 mm
Maximum Layers	10
Growth Rate	1,1
Inflation Algorithm	Pre

Fig. 7. Determination of wall layer size for selected domain and wall geometry in Ansys Mesh module.

defined within the range 1,05–1,1 for various zones. A finite element mesh sensitivity test was performed for the specified boundary conditions. The results of the test are shown in Fig. 8. As indicated in Fig. 8 satisfactory results of the selected parameters occur around $12{\cdot}10^6$ finite elements for this model. The conditions for the finite element mesh sensitivity test were defined by NASA (National Aeronautics and Space Administration) in the NPARC Alliance (National Program for Applications - Oriented Research in CFD) programme [16]. These conditions determine the order of mesh convergence, which determines the difference between the discrete solution and the exact solution. The convergence is defined by the GCI index - this is the percentage error of the results for the specified boundary conditions relative to the exact solution. The error defined by the smallest difference between successive simulations performed for a continuously increasing number of finite elements is considered the exact solution. The discrete geometric model used is shown in Figs. 9 and 10:

Carrying out a mesh quality test, enables observation of the obtained Yplus [12] values for the outer walls of the discrete model in the CFD-POST module used to develop the simulation results.

2.5. Results of calculations

The values of the set flow rate and the resulting differential pressure in the simulations are shown in Figs. 11 and 12. The simulation was performed according to the scheme described by the author in the publication [17]. Use the built-in value calculator in the CFD-POST module was used to determine the selected average parameters for the flow.

The selected parameters determined while testing.

- massFlow()@Boundary – mass flow rate for the selected boundary,
- ave(Velocity)@Boundary – average speed for the selected border,
- maxVal(Velocity)@Boundary – maximum speed value for the selected limit,

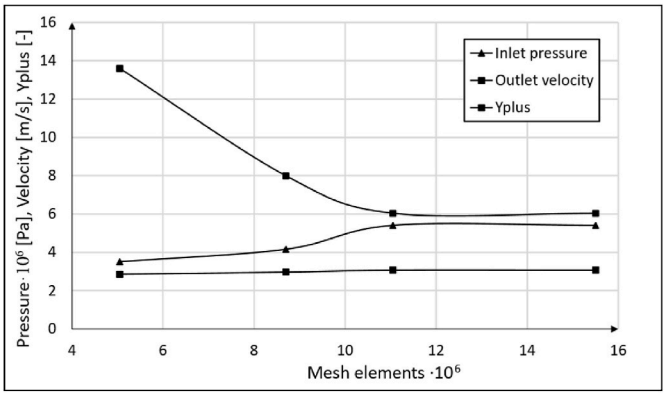

Fig. 8. Finite element mesh quality test results, In pressure (inlet pressure), Out velocity (outlet velocity), Yplus value.

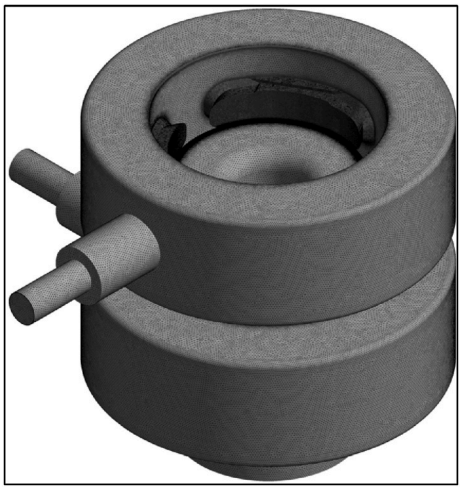

Fig. 9. Finite element mesh - isometric view.

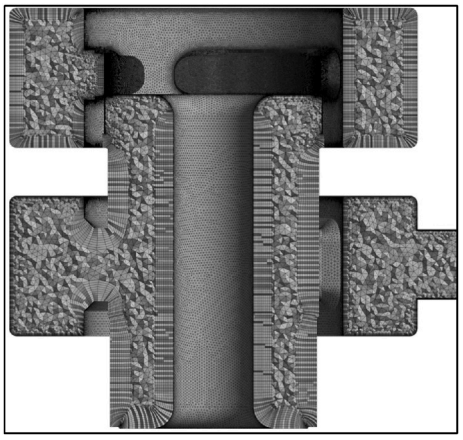

Fig. 10. Finite element mesh - model cross-section.

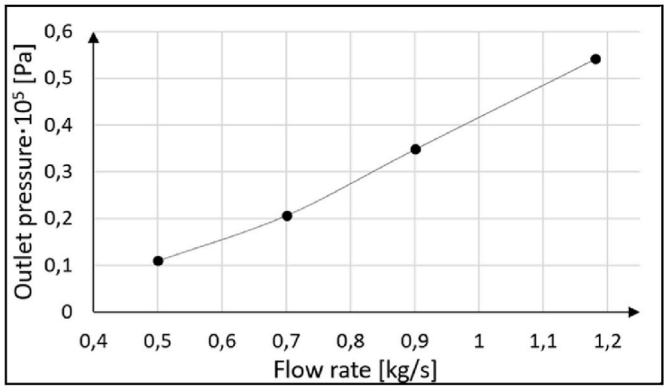

Fig. 11. Outlet pressure and flowrate for 25 % of opening.

- minVal(Velocity)@Boundary – minimum speed value for the selected limit,
- ave(Pressure)@Boundary – average pressure value for the selected limit.

Example of simulation results for an opening setpoint of 100 % and a flow rate of 7,27 kg/s is shown in Fig. 13. The change in the flow rate value and the change in the valve spool opening are manifested by the change in the angle of the stream outlet at the edge of the valve.

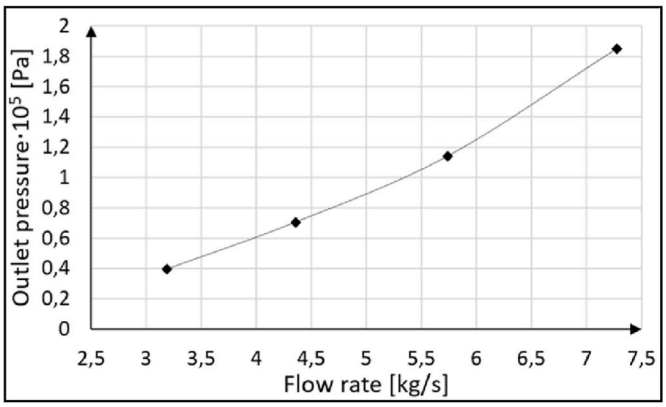

Fig. 12. Outlet pressure and flowrate for 100 % of opening.

2.6. Test bench, system diagram and measurement equipment

Laboratory tests of the flow divider located in the Institute of Power Engineering Gdansk division laboratory were carried out. For this purpose, a test bench was constructed consisting of.

- main proportional flow control valve;
- pilot valve;
- a PLC controlling the system, measurement frequency 100Hz,
- piston flowmeter, measurement range 0–15 kg/s, class 0,1;
- pressure transducers, measurement range 0–4·10^6 Pa, class 0,2.

For the validation of the simulation test, the bench tests were carried out. The diagram of the test bench is shown in Fig. 15 and the photo in Fig. 14.

2.7. Test results

For each degree of the opening of the proportional flow control valve, in the direction of flow through the ports P-B in the opening range of 0,001 m to 0,004 m (0–100 %), a pressure calibration was carried out at the outlet of the proportional flow control valve in order to determine the constant pressure drop in the component for different flow rates. For this purpose, a throttle valve was built into the test bench at the outlet of port B of the flow control valve (pressure marked as P2). The supply pressure was marked as P3 (this is the pressure at the air-oil tank station). The flow valve control pressure has been designated as P4 (this is the output pressure from the pre-control stage of the hydraulic valve). The opening setpoint of the main proportional flow control valve was marked as Value of task (ranging from 0 % to 100 % opening). The pressure distribution during test at 25 % of the opening is shown in Fig. 16. The characteristics of the dependence of the flow rate on the degree of the gap opening of the valve is shown in Fig. 17. The specified pressure drop of $\Delta p = 13$ bar was chosen due to the design of the test system. The tested system was powered by a hydraulic bladderless accumulator, where the vessel capacity equalled 2 m^3. With the assumed pressure difference, the largest resource of the hydraulic accumulator was obtained. This allowed performing tests of the flow rate through the valve in the full range of its opening, for a specified pressure drop. With a bigger pressure drop, the achieved flow rate would probably be much higher, which would shorten the time in which it is possible to measure the flow rate with the most constant conditions of the experiment. For the same reason, it was decided to perform simulation tests of the prototype valve with a lower pressure difference, so that it would be possible to perform bench tests for the available laboratory infrastructure.

Due to the design of the test stand, an attempt was made to obtain the most similar conditions for many measurements. However, considering the fact that a hydraulic accumulator was used as a compressed medium vesseland not a pressure pump with a p = constant regulator, it should be assumed that minor deviations from the established pressure drop during measurements could have occurred. However, they were not greater than 0,2·10^5 Pa.

As can be seen in Fig. 17 the flow characteristics has the features of linearity, but it is not proportional to the degree of the opening of the spool. The flow intensity appears at about 12 % of the spool opening degree. This is due to the spool design - the overlap in the sleeve is positive. The type of spool overlap affects the value of the pressure peak that occurs in the valve at rapid movement of the spool. For negative overlap in intermediate states, all channels of the valve are connected – this allows for gentle throttling of the flow in the transition phase and the pressure increase is gentle. For positive overlap, in intermediate states, all channels are cut off, which causes a more rapid increase in pressure once the channels are connected. The value of this pressure jump is also influenced by the size of internal leaks in the valve, deformation of hydraulic lines or the compressibility of the working medium (in hydro power engineering, systems powered by bladderless

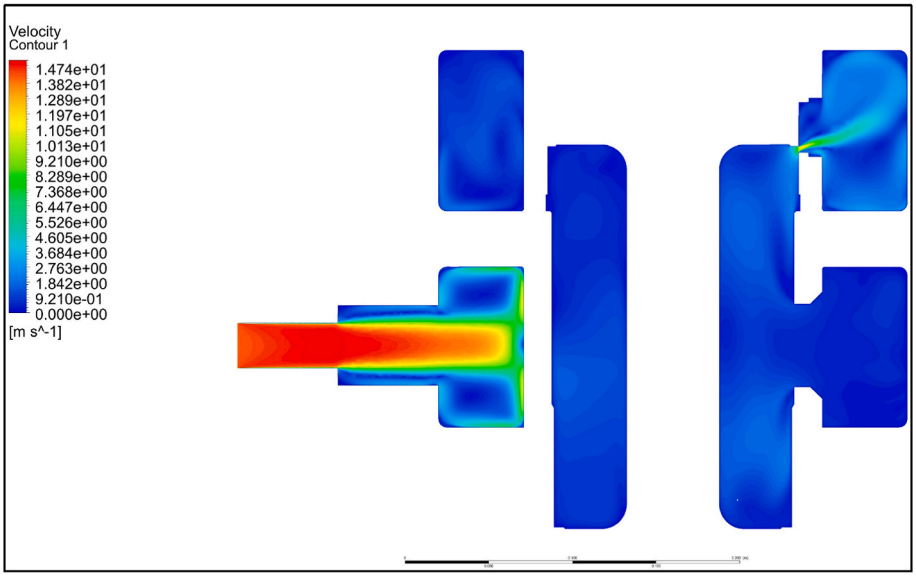

Fig. 13. Fluid velocity contour of the cross section passing through the P supply port.

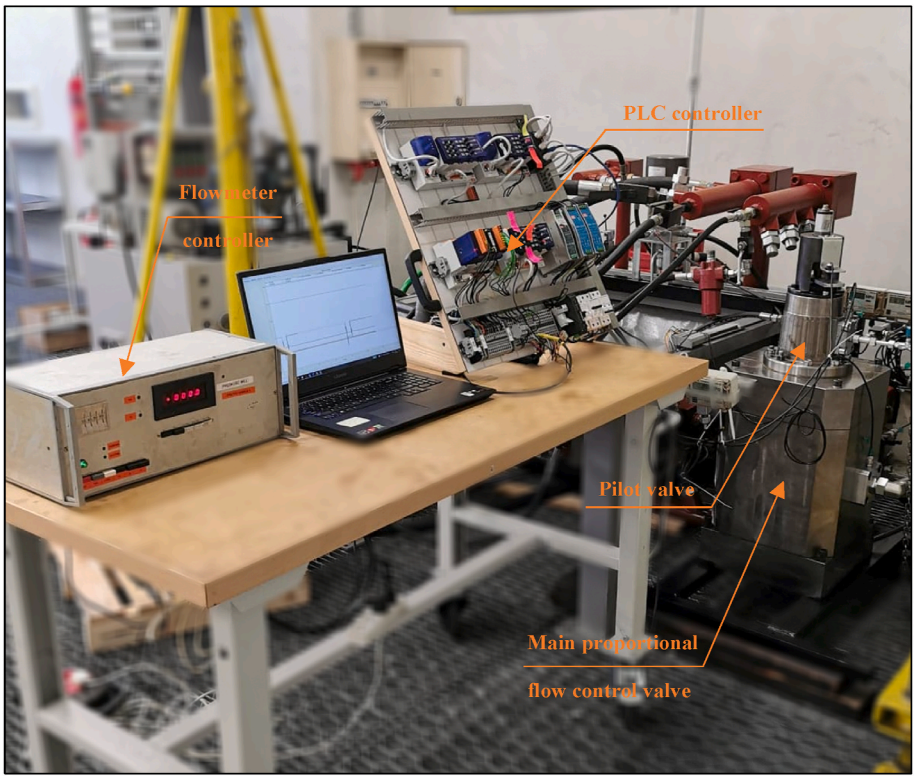

Fig. 14. Measurement bench during laboratory tests.

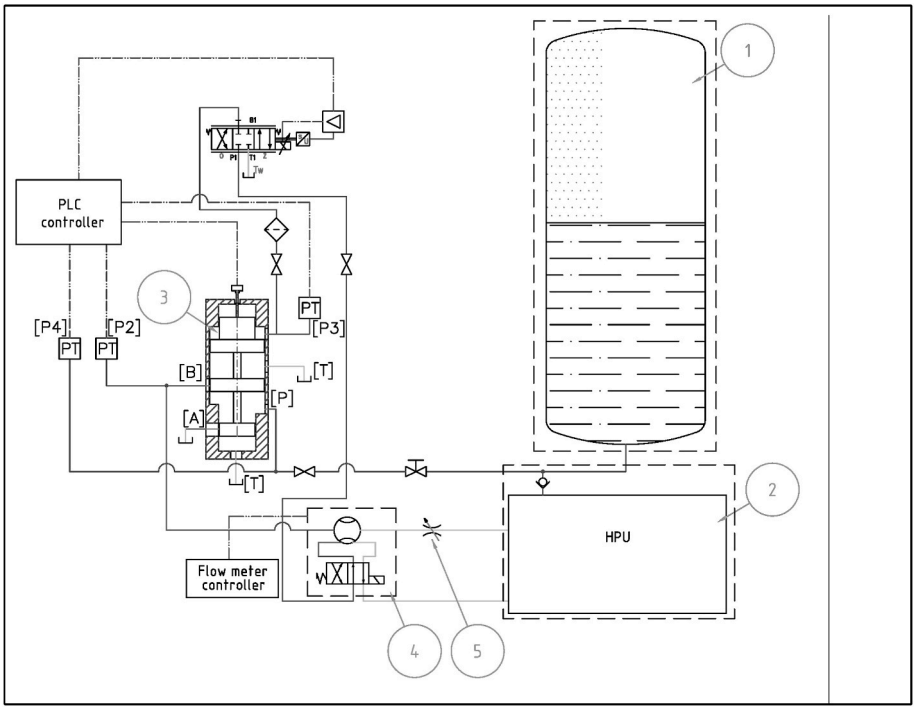

Fig. 15. Schematic diagram of the test bench; 1) Pressurized oil-air vessel, 2) HPU, 3) Hydraulic valve under test, 4) Piston flow meter, 5) Throttle valve.

hydraulic accumulators can often be found, where a certain amount of air is constantly dissolved in the hydraulic oil).

2.8. Comparison of the experimental results with results of numerical calculations

A comparison was made between the results obtained from the bench experiment and those obtained from a number of computer CFD simulations. Simulation methods have the unquestionable advantage of

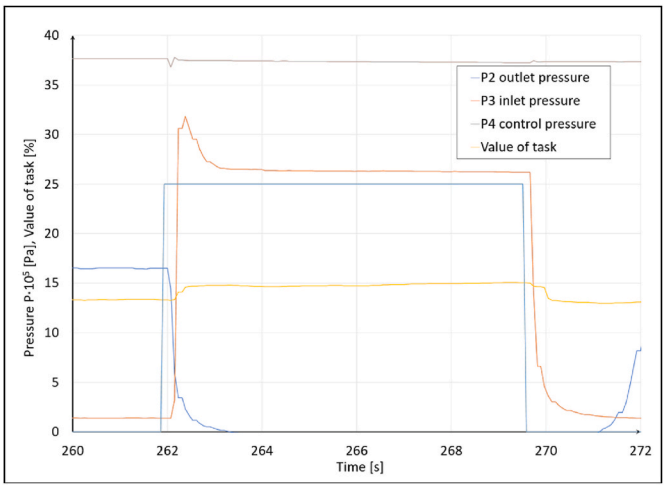

Fig. 16. Example of pressure distribution during flow rate measurement for a 25 % opening setpoint at a fixed pressure drop, P3 (Inlet pressure) - supply pressure, P2 (Outlet pressure) - pressure at the outlet of port B, P4 - control pressure, Val (Value of task) – an opening setpoint of the main control valve.

enabling the researchers the creation of any computational model, for any given boundary conditions, of any matter under any given conditions. No prototype or test bench is required.

The results obtained during the simulation tests Figs. 11 and 12 were compared with those obtained during the bench tests. For each given opening, simulations were performed for four different boundary conditions at the domain inlet. The result of the simulation is the resulting pressure at the inlet to the domain, which, unlike the pressure at the outlet, represents the pressure drop during flow through the valve. A graph showing a comparison of the results obtained by the two methods for a preset spool opening of 25 % is shown in Fig. 18. The biggest difference for a spool opening of 25 % was 9.8 % for the laboratory model. A graph comparing the results obtained by the two methods for a given spool opening of 100 % is shown in Fig. 19.

3. Proposal for a new proportional flow control valve design

Through a thorough analysis of fluid mechanics theory and the theory of hydraulic valve construction, as well as reading a number of scientific articles, assumptions have been formulated for the creation of a new fluid domain geometry for high-flow hydraulic valves, whose area of application is a hydro turbine control systems. Assumptions.

- minimizing the dimensions of the development in relation to the solutions used;
- two-sided support of the spool by the supply pressure, to force the tendency of the hydro-turbine to close in case of loss of control pressure;
- the flow rate at a supply pressure of less than $4{\cdot}10^6$ Pa and a pressure drop of $1{\cdot}10^6$ Pa in the flow element should be 15 kg/s;
- equipping the valve body with a sleeve (possibility of regenerating the element);
- connection duct size diameter of 0,048 m (average velocity in the supply port should not exceed 8 m/s for a flow rate of 15 kg/s;
- the design of the spool pair should have a positive or zero overlap.

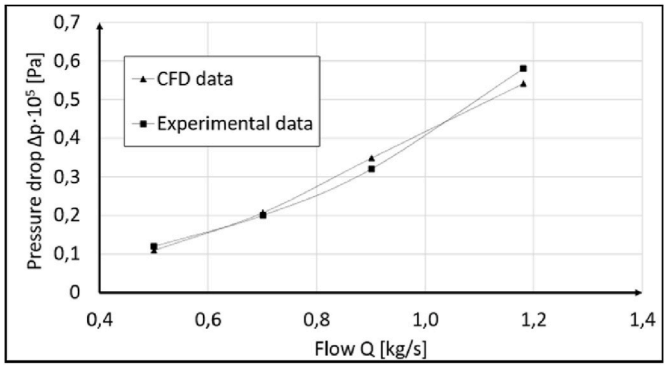

Fig. 18. Flow rate during simulation and experimental tests for a spool opening of 25 % P–B.

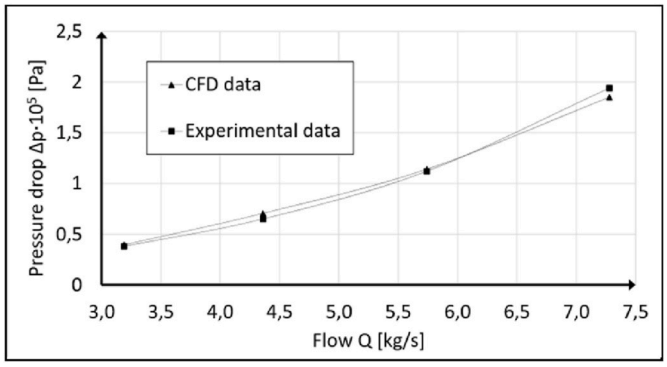

Fig. 19. Flow rate during simulation and experimental tests for a spool opening of 100 % P–B.

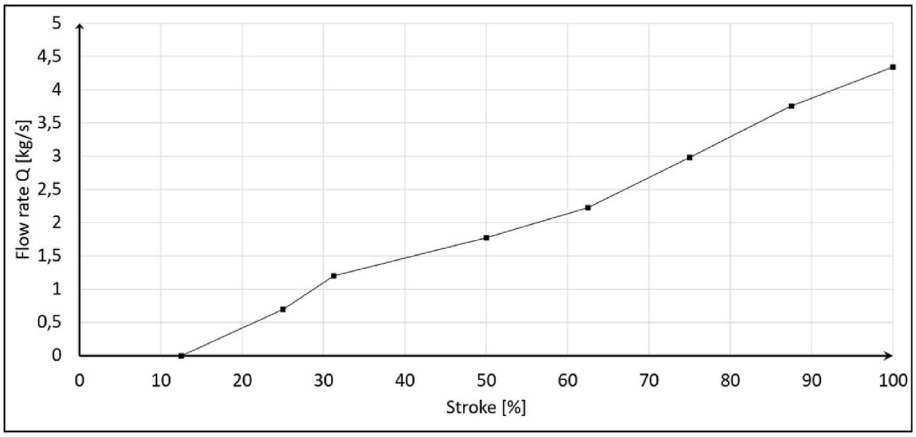

Fig. 17. Flow rate characteristic Q [flow in] as a function of the degree of the opening of the valve for a constant pressure drop $\Delta p = 13$ bar.

Improvements compared to the old solution.

- Changing the spool diameter from 0,15-0,142m to the 0,1-0,05m;
- Increasing the ratio of control surfaces (ensuring safe closing function of the wicket gate);
- Reducing the sensitivity of the system to contamination in the hydraulic system (separation of the control stage from the main stage, pressure supply to the control stage from another (compact) control unit;
- Introduction of grooves on the cylindrical surfaces to ensure axial pressure distribution along the surface of the spool and body (or sleeve). Currently, the lack of such a solution causes abrasion of the cylindrical surfaces of the spool and sleeve, which may consequently lead to its jamming and inability to operate.

3.1. Concept

The solution concept is presented in Fig. 20. The oil flow through the main valve is possible when the ports are connected.

a) P2-B3 (opening the wicket gate) + A3-T (return of the oil from the second port of the actuator when opening the wicket gate), in this situation the valve pilot is activated and the oil flows P1-A1, and then the pressure acts on the lower surface spool A2. On the opposite side there is the spool surface A4 powered by the lower pressure P3.
b) P2-A3 (closing the wicket gate) + B3-T (return of the oil from the second port of the actuator when closing the wicket gate), in this situation, the valve pilot connects the ports A1-T, and due to the difference in area A4 > A2 and the influence of low pressure on the A4 surface, the main proportional flow control valve spool is moved down.

Certainly, due to the fact that it is a proportional flow rate control valve, the degree of opening in a given flow direction directly affects the opening and closing speed of the wicket gate or the Kaplan turbine blade runner.

3.2. Geometry model

After an analysis of the assumptions, the geometry of the flow elements of the new main proportional flow control valve was created, as shown in Fig. 21 and Fig. 22.

3.3. Definition of boundary conditions

The calculations were carried out for two options.

- determination of the flow characteristics for a constant pressure drop of $\Delta p = 1{\cdot}10^6$ Pa;

The SST model was used to carry out the simulations. The boundary conditions (Fig. 23) for the determination of the flow characteristics were defined as.

- the pressure at the inlet to the domain is $3{,}8{\cdot}10^6$ Pa;
- the pressure at the domain outlet is $2{,}8{\cdot}10^6$ Pa - Opening boundary (for flow characteristics at constant pressure drop)
- the pressure at the domain outlet is 0 Pa - Opening boundary (for maximum pressure drop),
- frictionless flow (no-slip walls),
- isothermal.

3.4. Mesh model

The fluid volume filling the proportional flow control valve was then

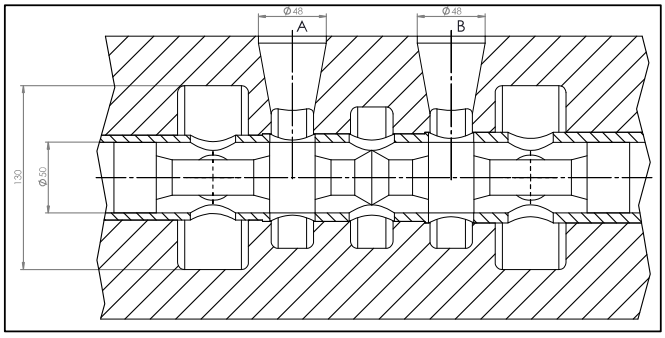

Fig. 21. Cross-sectional view of the geometry of the main control valve body, sleeve, spool in the plane passing through A,B ports.

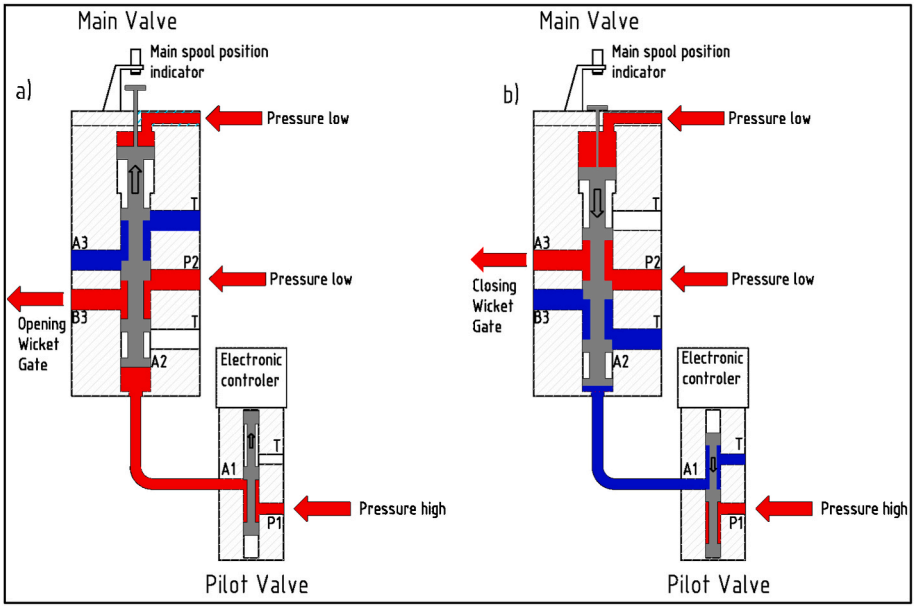

Fig. 20. Concept of the wicket gate control unit element. (a) control when opening the wicket gate, (b) control when closing the wicket gate.

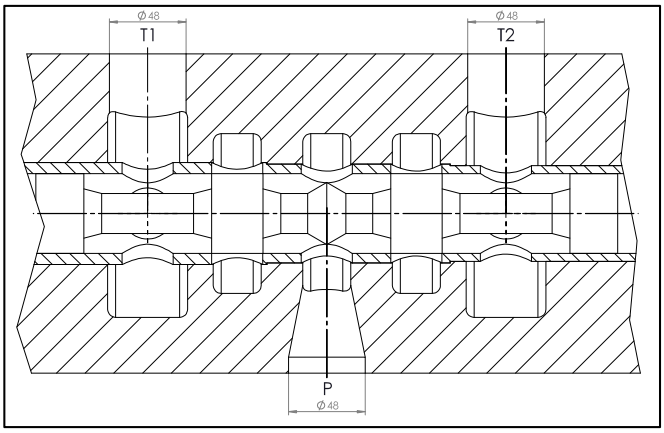

Fig. 22. Cross-sectional view of the geometry of the main control valve body, sleeve, spool in the plane passing through the ports P, T1, T2.

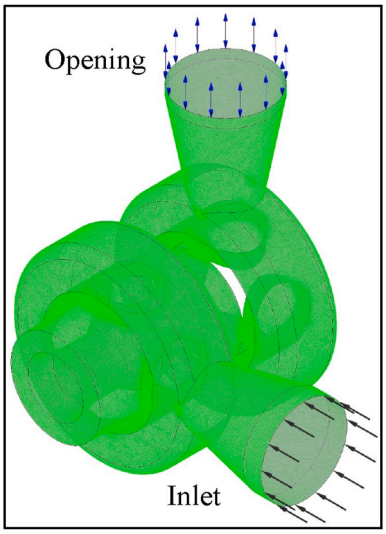

Fig. 23. Isometric view - boundary conditions defined in the CFX-PRE module.

created through a 3D modelling operation. The model was completely parameterized so that the spool stroke could also be inflicted in the CFD calculation software. The 3D model was imported into the Design Modeler module of Ansys Workbench. The imported parameters were incorporated and then one proceeded to create the discrete model in the Meshing module. The calculations were carried out for the flow through the P-B ports (the flow through the P-A ports is symmetrical with respect to the one presented).

The discrete model (Fig. 24) consists of 7902476 finite elements formed by 16608440 nodes. The 'Patch Conforming' mesh method with Tet10 tetrahedral elements was used. The use of wall layers also creates Wed15 and Pyr13 elements. The use of linear or quadratic elements was marked as controlled by the software. The global finite element size was set to 0,001 m and the maximum element size was set to 0,002 m. In the areas of greatest constriction in the model, a grid gradation of first $0{,}25{\cdot}10^{3}$ m and then $0{,}1{\cdot}10^{3}$ m was used (so that the minimum flow edge would consist of 10 elements for a spool opening of 0,001 m).

3.5. Results of calculations

Determination of flow characteristics for a constant pressure drop of $\Delta p = 1{\cdot}10^{6}$ Pa. In order to determine the flow characteristics at constant pressure drop, ten steady-state simulations were carried out for ten different spool opening values. The flow characteristics at constant

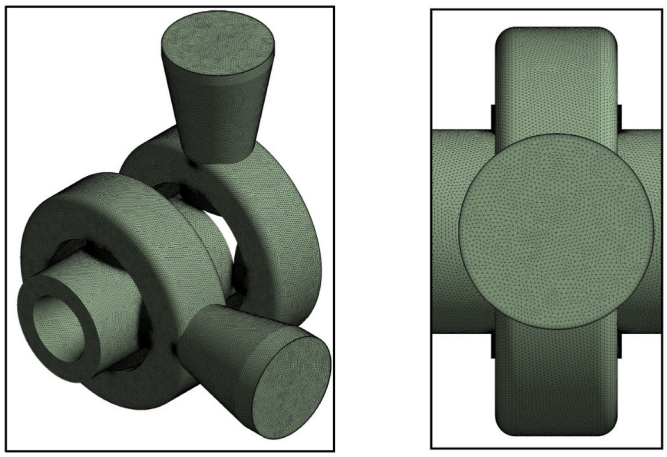

Fig. 24. Discrete flow valve model - isometric view and inlet plane view.

pressure drop are shown in Fig. 25.

As can be seen from the above characteristics, the flow rate is linear for flow rates between 2,23 and 14,13 kg/s. In order to achieve proportionality of the spool opening to the flow rate, it is still necessary to further optimize the flow chambers in the sleeve. The contours of the selected parameters for an opening of 10 % are shown in Figs. 26 and 27.

4. Comparison of the performance of the old and new flow control valve

At Fig. 28 comparison of two flow rate characteristics was presented.

- for the old solution, flow rate tests were carried out for a pressure difference of $\Delta p = 1{,}3{\cdot}10^{6}$ Pa;
- for the new solution, flow rate tests were carried out for a pressure difference of $\Delta p = 1{,}0{\cdot}10^{6}$ Pa;

The change in the specific pressure difference Δp during the tests is described in the "Test results" section below in this manuscript. As shown in Fig. 28, the new solution of a proportional control valve is characterized by significantly higher efficiency over the entire opening range and a practically linear opening characteristic from 10 % to 80 %. Over the entire range, the increase in efficiency is more than 300 % with a clear reduction in the dimensions of the control spool and body.

5. Methodology of design control valves for high flow rates

An original graph was developed and presented in Fig. 30, which is a methodology for designing control valves for high flow rates. It is a

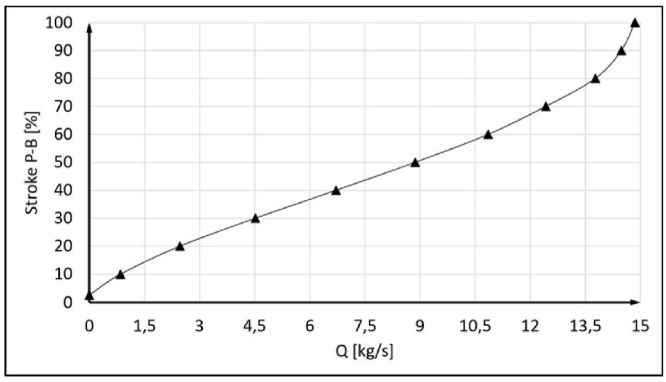

Fig. 25. Flow rate characteristics for spool openings in the range 0–100 % P–B for a constant pressure drop.

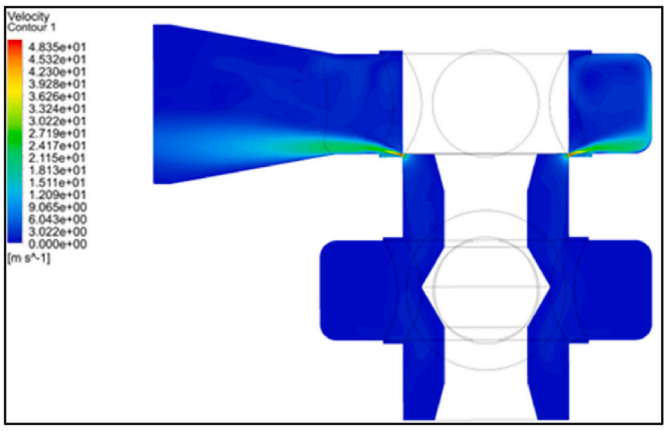

Fig. 26. Fluid velocity contour of the cross-section passing through B port.

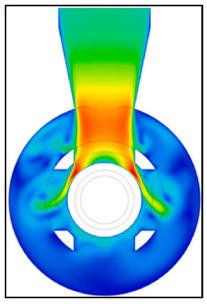

Fig. 27. Fluid velocity contour in cross-section normal to the axis of the valve, passing through the P supply port.

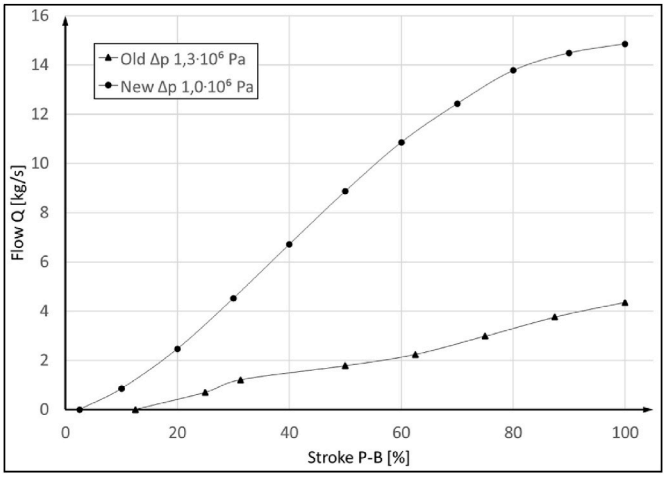

Fig. 28. Comparison of flow rate characteristics depending on the opening, at a constant pressure difference for the old and newly developed solution.

universal method and can be freely modified depending on the needs. Nevertheless, it presents a general scope of procedure for prototyping new solutions. The description of geometrical quantities used in the diagram is presented in Fig. 29.

6. Design of the prototype

Based on the diagram shown at Fig. 30 the new geometry of the CFD model was development, shown at Figs. 21 and 22. Due to CFD research the flow characteristic of the element shown at Fig. 25 was determined. The CFD tests confirmed the validity of the assumptions made, which

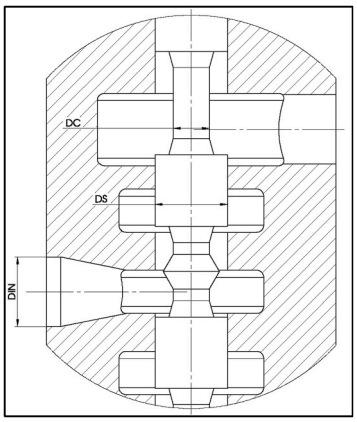

Fig. 29. Description of geometric quantities for the universal methodology for prototyping control valves.

were the basis for the development of the technical documentation for the prototype, shown at Fig. 31.

7. Conclusions

A theoretical analysis of all physical processes in the field of fluid mechanics and CFD simulation calculations occurring in the computational model were conducted. A CFD computational model was built based on the documentation of the existing main proportional flow control valve located at the laboratory of the Institute of Power Engineering, Polish National Institute, Gdansk division. The test results were collated and the correction factor w_c was determined. The innovation of this article consists in the analysis of the methodology of laboratory tests and those conducted through CFD simulation. Additionally a universal graph that can help other researchers in creating new structures has been described. The biggest difference of achieved pressure at the outlet was nearly 10 % for the laboratory model. Influence on the divergence of test results is exerted by the following factors.

- inaccuracy of measuring apparatus (pressure transducers, flow meter);
- difficulty in obtaining an accurate pressure drop during laboratory tests (there were slight deviations in pressure values in the valve outlet port);
- linear and local pressure losses in the hydraulic system;
- change in the physical and chemical properties of the working fluid due to wear;
- wear and tear on the main proportional flow control valve - perhaps the effect of years of operation is wear and tear on the control edges, for example;
- inaccuracy of the computational model (assumptions made, computational model, turbulence model, boundary conditions).

On the basis of the carried out tests, it can be assumed that the measurement uncertainty coefficient for the pressure loss in the component under test is.

- for flow rates up to the 15 kg/s, coefficient $w_c = 1{,}1$.

In further consideration of the new solution, the coefficients will be determined when analyzing the results of the CFD simulation studies. Comparing the results of the study to other publications [6,7] other researchers come to similar conclusions that the results of CFD tests compared to the validation of actual computational models do not exceed differences of 10 %.

A new geometry and concept of the main control valve was created. A series of CFD simulation studies were carried out and the flow

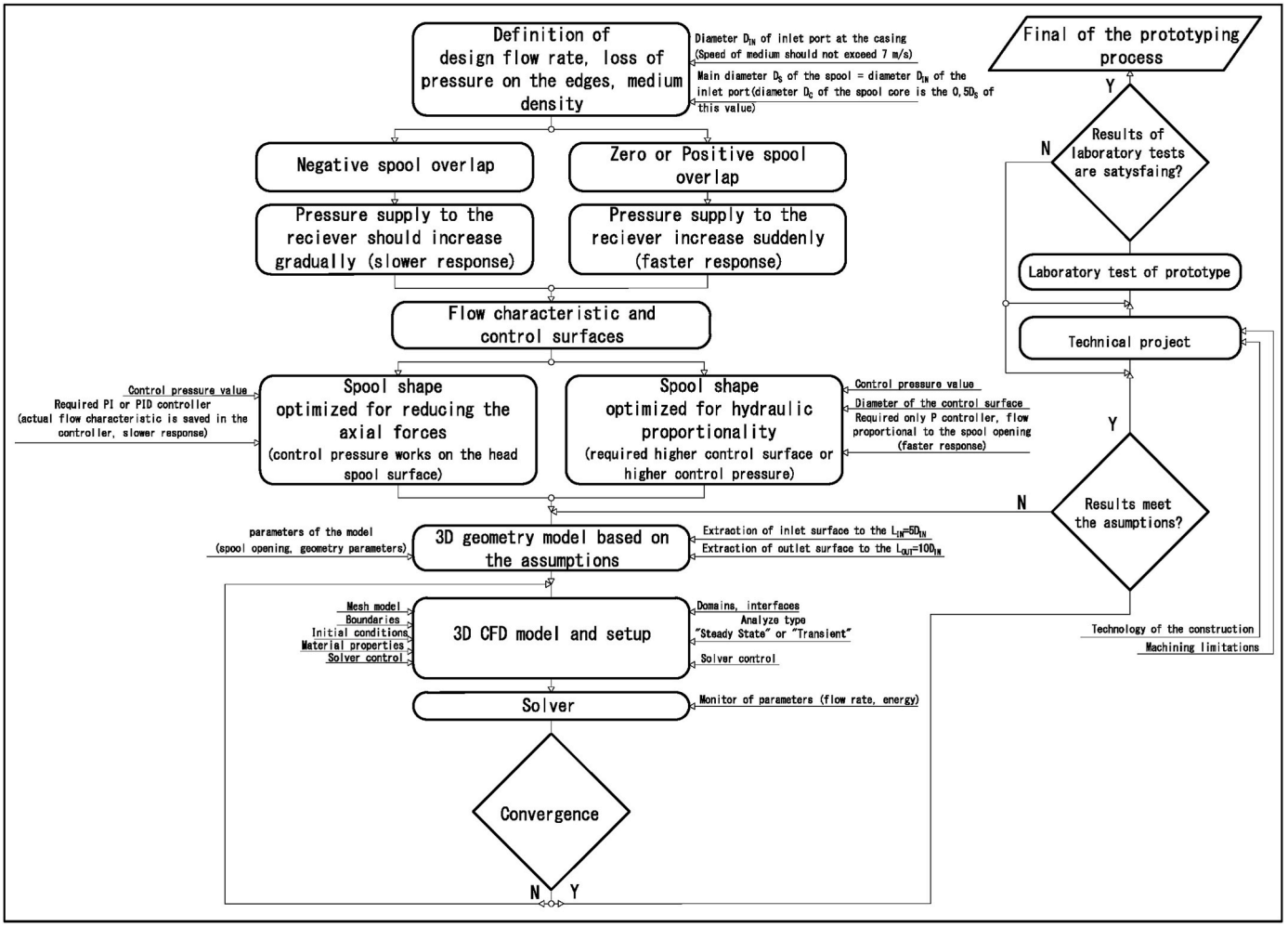

Fig. 30. Flowchart for the universal method for prototyping hydraulic control valves.

characteristics were determined for the opening over the entire range for flow through ports P-B (ports P-A are symmetrical) at a constant pressure drop. The flow rate at maximum pressure drop (determination of maximum flow rate) was simulated for the new proportional flow control valve geometry. The resulting flow characteristics (Fig. 25) shows linear characteristics for flow rates in the range 2,23 to 14,13 kg/s for a constant pressure drop of 1,0·106 Pa. The flow rate characteristics of the newly developed element were compared to the ones of the element currently in use, shown in Fig. 28. The new element characteristics is linear within 10 %–80 % of the opening and provides over 300 % increase in flow rate performance over the entire range at comparable, constant pressure drop. In the new solution, spool diameter is 0,05 m and if it were compared with the old solution, where it was 0,14 m it is 280 % smaller than the diameter of the spool. It ensures that the lower inertia mass has a positive influence on faster response and dynamics.

8. Future works

The next stage of work will be to optimize the geometry of spool and cover for presented new geometry of the main proportional flow control valve. The authors assume obtaining the hydraulic proportionality relation of opening for achieved flow rate. The prototype will be produced and research validation of numerical CFD research will be shown. Next, the solution of a new control pilot for the operation in a low-flow control circuit using a higher supply pressure will be presented. This will be followed by optimization of the interaction of the new main proportional flow control valve with the control element in terms of static and dynamic control parameters of the HPU system.

CRediT authorship contribution statement

Mateusz Kosek: Writing – review & editing, Writing – original draft, Visualization, Software, Methodology, Investigation, Formal analysis, Data curation, Conceptualization. **Dariusz Downar:** Supervision, Funding acquisition. **Pawel Sliwinski:** Validation, Supervision.

Data availability

The datasets generated and/or analyzed during the current study are not publicly available due to protection of the solutions presented in the article but are available from the corresponding author on reasonable request.

Declaration of competing interest

The authors declare the following financial interests/personal relationships which may be considered as potential competing interests: Mateusz Kosek reports financial support was provided by Institute of Power Engineering. Mateusz Kosek reports a relationship with Institute of Power Engineering that includes: employment. Dariusz Downar reports a relationship with Institute of Power Engineering that includes: employment. If there are other authors, they declare that they have no known competing financial interests or personal relationships that could have appeared to influence the work reported in this paper.

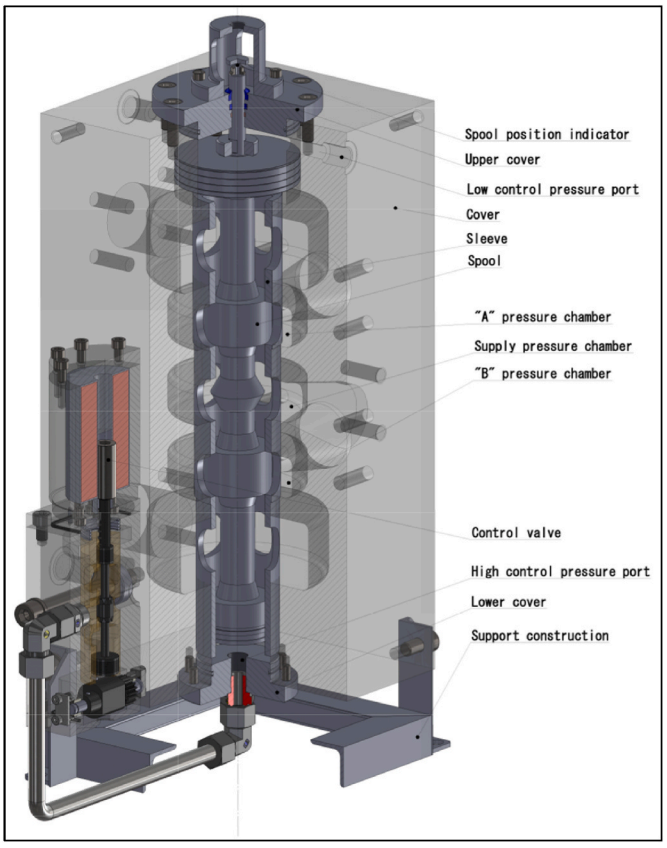

Fig. 31. Prototype of the main proportional flow control valve with the control stage – isometric cross-section view.

Data availability

Data will be made available on request.

References

[1] G. Chang Lei, Y.X. Tianhang, W. Tuerxun, An improved mayfly optimization algorithm based on median position and its application in the optimization of PID parameters of hydro-turbine governor, IEEE Access 10 (2022), https://doi.org/10.1109/ACCESS.2022.3160714.
[2] X. Pan, & others. Stability analysis of hydro-turbine governing system with sloping ceiling tailrace tunnel and upstream surge tank considering nonlinear hydro-turbine characteristics, Renew. Energy 210 (2023), https://doi.org/10.1016/j.renene.2023.04.028.
[3] L. Yongyao, others, Multibody dynamics analysis of a Kaplan turbine runner in full operating conditions, J. Energy Storage 72 (2023), https://doi.org/10.1016/j.est.2023.108269.
[4] A. Chamil, Modelling and optimisation of a Kaplan turbine — a comprehensive theoretical and CFD study, Cleaner Energy Systems 3 (2022), https://doi.org/10.1016/j.cles.2022.100017.
[5] Directional control valves, direct operated, with electrical position feedback and integrated electronics (OBE) Type 4WRLE. RE 29123 Rexroth a Bosch company. https://store.boschrexroth.com/Hydraulics/Valves/Directional-valves/Proportional-directional-valves?cclcl=en_US&optly_variant=version1, 2023.
[6] R. Amirante, E. Distaso, P. Tamburrano, Experimental and numerical analysis of cavitation in hydraulic proportional directional valves, Energy Convers. Manag. 87 (2014), https://doi.org/10.1016/j.enconman.2014.07.031.
[7] K. Sharipov, S. Mirzaliev, Simulation of a hydraulic load sensing proportional valve, Preprints (2018). https://doi:10.20944/preprints201810.0242.v1.
[8] White, Frank M. Fluid Mechanics fourth ed., University of Rhode Island.ISBN: 978-0072281927.
[9] Versteeg, H. K. & Malalasekera, W. An Introduction to Computational Fluid Dynamics second ed. ISBN: 978-0-13-127498-3.
[10] S.W. Choi, H.S. Seo, H.S. Kim, Analysis of flow characteristics and effects of turbulence models for the Butterfly valve, Appl. Sci. 11 (2021) 6319, https://doi.org/10.3390/app11146319.
[11] N.L. Scuro, E. Angelo, G. Angelo, D.A. Andrade, A CFD analysis of the flow dynamics of a directly-operated safety relief valve, Nucl. Eng. Des. 328 (2018), https://doi.org/10.1016/j.nucengdes.2018.01.024.
[12] K. Chitale, O. Sahni, S. Tendulkar, N. Rocco, M. Shephard, K. Jansen, Boundary layer adaptivity for transonic turbulent flows, 21 AIAA Computational Fluid Dynamics Conference (2013), https://doi.org/10.2514/6.2013-2445.
[13] C. Johansson, Optimization of Wall Parameters Using CFD, Royal Institute of Technology, 2014. https://www.diva-portal.org/smash/get/diva2:787495/FULLTEXT01.pdf.
[14] SolidWorks 2020 User's Guide.
[15] Ansys Help 2022 R2.
[16] Examining Spatial (Grid) Convergence. https://www.grc.nasa.gov/www/wind/valid/tutorial/spatconv.html.
[17] M. Kosek, CFD simulation of kaplan turbine rotating union and the development of a real time diagnostic system, International Review on Modelling and Simulations (I.RE.MO.S.) 5 (2021) 14, https://doi.org/10.15866/iremos.v14i5.21217.